Sky View Factors from High-Resolution Scanned Fish-eye Lens Photographic Negatives

KRISTINA BLENNOW

Department of Physical Geography, Lund University, Sweden

28 September 1994 and 10 April 1995

ABSTRACT

A computerized method for calculating the sky view factor from fish-eye lens photographic negatives is presented. The images are scanned and stored on CD ROM, each CD holding 100 images. The images can be retrieved at very high resolutions of up to 2048 × 3072 pixels for one 24 mm × 36 mm negative. The calculations include corrections for lens projection distortion and restrictions in field of view. They are compared to standard methods of calculating the sky view factor. For applications of the sky view factor where the effective infrared radiation is of interest, a method to account for zenith angular variation in atmospheric transmissivity to infrared radiation is presented.

1. Introduction

Fish-eye lens photography is widely used for characterization of radiation conditions when parts of the sky are obscured by objects such as vegetation canopies or buildings. In this way the incident direct and diffuse solar radiation, as seen from a point, can be estimated by plotting the solar path on photographs and by examining the relation between unobscured and obscured parts of the sky (e.g., Anderson 1964). The exchange of diffuse radiation between two surfaces can be expressed as a geometrical factor called the view factor, angle factor, shape factor, or configuration factor and was derived by, for example, Reifsnyder (1967) for radiating surfaces separated by a transparent medium. The sky view factor expresses the radiative exchange between a small area and the unobscured part of the sky above. Based on the concept of view factor for a transparent medium, Steyn (1980) and Steyn et al. (1986) developed methods for calculation of the sky view factor from fish-eye lens images. Calculated using the former method, the sky view factor has been used to assess the effective infrared radiation conditions on clear and calm nights in urban canyons (e.g., Bärring et al. 1985; Eliasson 1992; Oke 1981) and in more complex environments such as beneath forest canopies (e.g., Nunez and Sander 1982).

Previously published methods for determining various view factors and indices from fish-eye lens photographs make use of positive copies of the photographs for manual analysis (e.g., Steyn 1980) or digitizing followed by computerized analysis (e.g., Chen et al. 1991). Chan et al. (1986) used a light sensor for sampling the light intensity of the image from the negative projected through a lens system. Olsson et al. (1982), however, used a scanner for digitizing negatives yielding a maximum of 1024 × 1024 pixels. In order to reduce the computing time, the calculations were performed after retrieving the image in reduced resolution in an array of 512 × 512 pixels. Becker et al. (1989) used a video camera and a digitizer to produce images from negatives in an array of 485 × 572 pixels. The sky view factor has been calculated from digitized positive paper copies using a video camera followed by computerized image analysis (Bärring et al. 1985). Steyn et al. (1986) used a frame-store device to digitize images produced by a video camera equipped with a fish-eye lens. In this way the circular image was reproduced within a 256 × 256 array of rectangular pixels.

Steyn's method for computing the sky view factor, a modified version by Johnson and Watson (1984), and the method presented by Steyn et al. (1986) were designed for equiangular projections. However, these methods do not take into account lens specific deviations from perfectly equiangular projections as produced by commercially available fish-eye lenses (Herbert 1987). Also, the field of view for fish-eye lenses varies and often deviates from 180° (Clark and Follin 1988; Evans et al. 1975). When tracking solar paths and calculating view factors and canopy indices, such as the leaf area index, from fish-eye lens images, the lens projective properties including distortion (Becker et al. 1989) and restriction in field of view must be considered.

Calculated using the Steyn (1980) method, the sky view factor has been used for effective infrared radiation applications disregarding the fact that air is not completely transparent to infrared radiation due to its con-

Corresponding author address: Kristina Blennow, Department of Physical Geography, Lund University, Sölvegatan 13, S-223 62 Lund, Sweden.

tent of particulate material and greenhouse gases such as carbon dioxide and the more varying content of water vapor. For an unobscured clear sky the infrared radiation transmissivity varies with zenith angle notably due to differences in water vapor content (Unsworth and Monteith 1975). The transmissivity is greatest, and hence the atmospheric counter radiation is least, in directions near the zenith. This should be taken into account for applications where the effective infrared radiation is of interest.

Heavy demands on available computer memory for storing digitized images can be met by using compact disk read-only memory (CD ROM). In this paper, scanning, storing, and retrieving very high resolution digital images from fish-eye lens photographic negatives are presented. Also, methods for correcting for lens projection distortion and restrictions in field of view as well as the varying transparency of air to infrared radiation are presented for calculation of the sky view factor. A comparison is made between the sky view factor calculated using the Steyn method modified by Johnson and Watson (1984), the lens projection corrected sky view factor, and the latter factor compensated for the effect of greenhouse gases on the zenith angular infrared radiation transparency of the air.

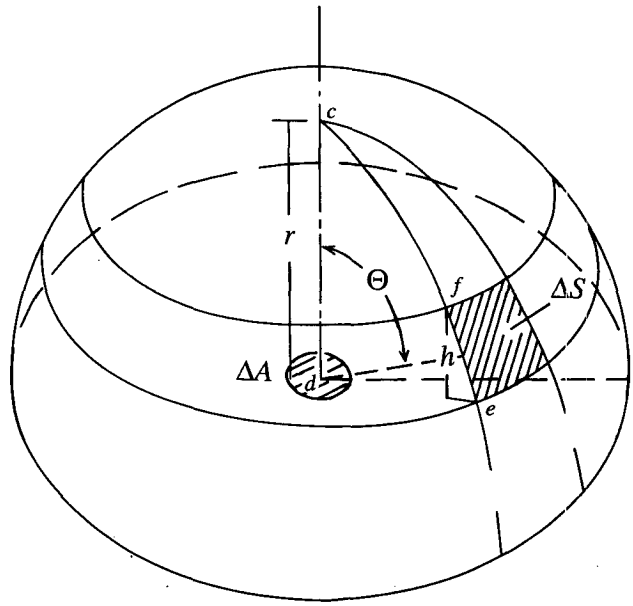

FIG. 1. Graphical representation of the view factor. Here θ is the zenith angle of the middle (by angle) of the annulus, the angles *cde* and *cdf*, denoted θ_1 and θ_2, respectively, in the text, correspond to the zenith angles of the edges of the annulus, and h is the height of the annulus. Modified from Johnson and Watson (1984).

2. Sky view factors from fish-eye lens images

The total diffuse radiation flux E from a small surface area ΔA is given by

$$E = \pi I_n, \tag{1}$$

where I_n is the intensity of the radiation in the normal direction. As shown by Reifsnyder (1967), the view factor Γ from ΔA for a small area ΔS on the hemisphere can be expressed as

$$\Gamma = \frac{\Delta E}{E} = \frac{I_n \Delta S \cos\theta}{I_n \pi r^2} = \frac{\Delta S \cos\theta}{\pi r^2}, \tag{2}$$

where θ is the zenith angle and r is defined in Fig. 1. The sky view factor Ψ for the small surface area ΔA is the fraction of diffuse radiation leaving ΔA and reaching the sky represented by the hemisphere. Also, the reciprocal case holds; the fraction of diffuse radiation reaching ΔA from the sky to the total amount of diffuse radiation from an unobscured sky equals Ψ.

Steyn's (1980) method for calculation of the sky view factor is based on dividing the projected image into annuli of equal width. In the modified version by Johnson and Watson (1984) the factor can be calculated exactly over each annulus in an equiangular projection. The sky view factor Ψ can, however, be calculated from most projections produced by standard fish-eye lenses but measures to correct from projection distortion must be taken. This can be done using the expression of Johnson and Watson (1984) but dividing the image into annuli of equal latitudinal angular widths where the corresponding width of each annulus on the projected image can be calculated from a lens-specific projection formula. In order to maximize the available number of annuli for calculation of the sky view factor, however, the following approach is taken. The area S_i of an annulus on the hemisphere is given by

$$S_i = 2\pi r h, \tag{3}$$

where r and h are defined in Fig. 1. Here h can be expressed as

$$h = r(\cos\theta_2 - \cos\theta_1), \tag{4}$$

where θ_1 and θ_2 are the zenith angles corresponding to the edges of the annulus (Fig. 1). The area of the sky part of the ith annulus is thus

$$S_{i,\text{sky}} = 2\pi r^2(\cos\theta_2 - \cos\theta_1)\frac{m_i}{t_i}, \tag{5}$$

where m_i is the number of sky pixels and t_i is the total number of pixels in the ith annulus. The sky view factor is given using (5) in (2) and summing for all annuli:

$$\Psi = 2\sum_{i=1}^{n} \cos\theta(\cos\theta_2 - \cos\theta_1)\frac{m_i}{t_i}, \tag{6}$$

where θ, θ_1, and θ_2 can be calculated from a lens-specific projection formula after distance measurements on the projected image. Corresponding corrections can be applied to the Steyn et al. (1986) method for calculating

the sky view factor where the calculations are made for individual pixels rather than for annuli. Program code for the initial method is given in Johnson (1990). For images of homogeneous canopies produced with lenses with fields of view less than 180°, the annulus approach makes it possible to approximate the m_i/t_i ratio for the part of the hemisphere that is outside the field of view of the lens by fitting a polynomial to the m_i/t_i ratio for zenith angles within the field of view and extrapolating the m_i/t_i ratios up to 90°.

3. Sky view factor for effective infrared radiation applications

View factors for a transparent medium are often used for conditions where the medium separating the radiating surfaces is not perfectly transparent to the wavelength band under consideration, such as when infrared radiation is transmitted through air. However, for such applications of the sky view factor the zenith angular variation in atmospheric transparency to infrared radiation (Fig. 2) should be accounted for. In an unobscured clear sky the atmospheric emissivity varies with zenith angle according to

$$\epsilon_\theta = a + b \ln(u \sec\theta), \tag{7}$$

where ϵ_θ is the emissivity in the zenith angle θ, u (cm) is the zenith optical path, and a and b are coefficients dependent on atmospheric stability and content of particulate material (Table 1) (Unsworth and Monteith 1975). The zenith optical path may be calculated from radiosonde data or approximated using an empirical relationship such as

$$\log u = 0.295(e^{1/2}) - 0.803 \tag{8}$$

for characteristic air masses over the British Isles, where u is in centimeters and e is the vapor pressure in hectopascals at the surface (Monteith 1961). Radiation reaching any "gray" object is either absorbed, transmitted, or reflected:

$$\gamma_\lambda + \tau_\lambda + \rho_\lambda = 1, \tag{9}$$

where γ_λ is the absorptivity, τ_λ is the transmissivity, and ρ_λ is the reflectivity for a specific wavelength λ. Using Kirchhoff's law,

$$\gamma_\lambda = \epsilon_\lambda, \tag{10}$$

where ϵ_λ is the emissivity for a specific wavelength; approximating the infrared radiation reflectivity of air to zero, the radiation fluxes, ΔE and E, in (2), are corrected for varying atmospheric transmissivity to infrared radiation by multiplying with $(1 - \epsilon_\theta)$ and $(1 - \epsilon_{\text{hemisphere}})$, respectively, where $\epsilon_{\text{hemisphere}}$ is the emissivity integrated over the entire hemisphere. As shown by Unsworth and Monteith (1975), the emissivity of a cloudless sky at a zenith angle of 52.5° equals $\epsilon_{\text{hemisphere}}$. Applying these corrections on the sky view factors for the consecutive annuli and summing for all annuli, the sky view factor Ψ_e for effective infrared radiation applications is produced:

$$\Psi_e = \frac{2}{(1 - \epsilon_{\text{hemisphere}})} \sum_{i=1}^{n} \cos\theta(\cos\theta_2 - \cos\theta_1) \times \frac{m_i}{r_i}(1 - \epsilon_\theta). \tag{11}$$

TABLE 1. Values of the coefficients a and b in the equation $\epsilon(\theta) = a + b \ln(u \sec\theta)$ as measured in the English Midlands with the number of observations in parentheses. Data from Unsworth and Monteith (1975).

Situation	a	b
Inversions (5)	0.71 ± 0.05	0.082 ± 0.004
Lapse (11)	0.67 ± 0.03	0.094 ± 0.003
All occasions (46)	0.70 ± 0.05	0.090 ± 0.002

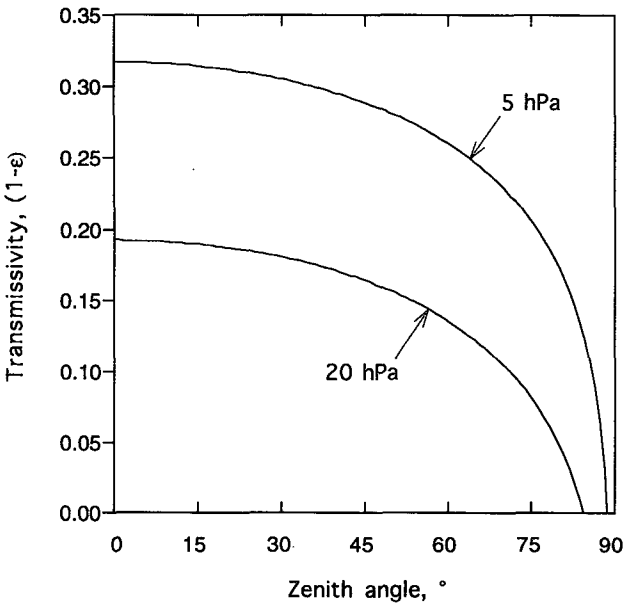

FIG. 2. The transmissivity $(1 - \epsilon_\theta)$ of the sky for various zenith angles θ at two surface vapor pressures. Calculated using Eq. (8) for situations with strong inversion, the zenith optical water path is 0.72 and 3.3 cm, corresponding to a surface vapor pressure of 5 and 20 hPa, respectively. Based on Unsworth and Monteith (1975).

4. Image generation and analysis

a. *Image generation*

Fish-eye lens photographs were taken in a mature forest of *Picea abies* Karst. L. in Tönnersjö Experimental Forest, south Sweden. The camera was attached to a tripod, and photographs with the lens facing upward were taken after careful horizontal positioning by use of a libel mounted on the lens. The exposure

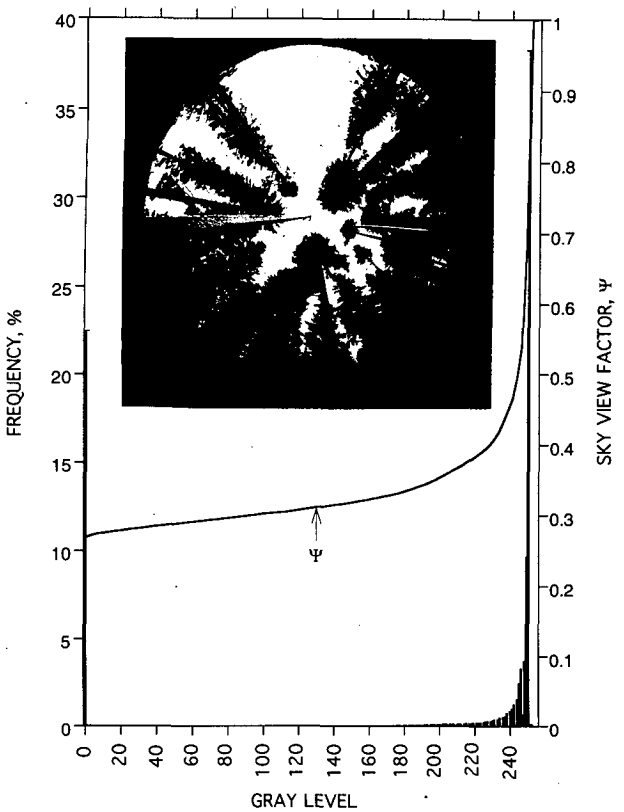

FIG. 3. The frequency of different gray levels within one circular image and the sky view factor Ψ for different threshold levels. The arrow represents a threshold level midway between black and white. Few pixels have gray values in the midrange between white and black and the corresponding blocks do not show well in the figure. The data-compression procedure included in the Kodak Photo CD system reduces the frequency of some gray-level values appearing as missing blocks in the figure.

settings and film were chosen so as to produce high-contrast images. Fine-grain Kodak Technical Pan film was exposed at ISO 100 after determining the exposure settings by measuring toward the sky with a separate Ashai Pentax spot exposure meter. The base of this film is made of polyester to make it insensitive to expansion due to humidity and temperature variations and thereby suited for distance measurements. The exposed film was developed using Kodak D 76 1:1 developer, and the negatives were scanned onto and stored in 256 gray levels on Kodak Photo CDs (Blennow 1994), each CD holding 100 images. According to the manufacturer, the data-compression procedure included in the system, however, reduces the frequency of some gray-level values appearing as missing blocks in Fig. 3. This has no practical importance for the calculation of view factors. The photographs were taken during overcast weather conditions using a Nikon 8-mm f/2.8 lens that projects an approximately equiangular circular image on the film plane. Based on Herbert (1986, 1987), a sixth-order polynomial was fit to calibration data presented by the manufacturer:

$$y = 0.140\theta - 4.419 \times 10^{-5}\theta^2 + 7.654 \times 10^{-7}\theta^3 - 6.672 \times 10^{-8}\theta^4 + 9.094 \times 10^{-10}\theta^5 - 4.284 \times 10^{-12}\theta^6, \quad (12)$$

where y (mm) is the distance between the center of the picture and any point on the circular image on the 24 mm × 36 mm negative and θ is the zenith angle in degrees. Laboratory tests using a comparator (Jena, Germany) confirm the field of view of 180° stated by the manufacturer at an aperture setting of 2.8. At other aperture settings the diameter of the image and the field of view are slightly decreased (Table 2).

b. *Image analysis*

The image can be retrieved from the Kodak Photo CD in five resolutions ranging from 128 × 192 to 2048 × 3072 quadratic pixels for one 24 mm × 36 mm negative. In the highest resolution the diameter of one circular image taken with the Nikon lens at f/5.6 corresponds to 2004 pixels. The image analysis was performed on scanned negatives using NIH Image 1.56b9 software that was run on a Power Macintosh 8100/80 computer with 41 Mbyte of internal memory. The images were converted to binary, that is, reproduced as true black and white, by selecting a threshold value between black and white. All pixels with gray levels above this level were considered black, that is representing a sky-obscuring element, and all pixels with gray levels below this level were considered white, that is, representing an unobscured sky. The images should have high contrast and be retrieved in high resolution in order to minimize errors imposed from thresholding on the calculated sky view factor. Following Steyn et al. (1986), the threshold value was selected midway between black and white (Fig. 3). The number of "sky pixels" and the total number of pixels in each annulus were calculated and the distance measured between the center of the image and the center and edges of each annulus. The zenith angle corresponding to each annulus was calculated using (12). The field of view for the Nikon lens used in this study excludes only 0.3°

TABLE 2. The diameter of the image produced by Nikon 8-mm f/2.8 lens for all available aperture settings. The measurements were made using a comparator (Jena, Germany), and the corresponding fields of view were calculated from a sixth-order polynomial fit to calibration data presented by the manufacturer.

Aperture	Diameter (mm)	Field of view (°)
2.8	23.01	179.9
4	22.98	179.7
5.6	22.95	179.4
8	22.92	179.1
11	22.90	179.0
16	22.89	178.9
22	22.89	178.8

TABLE 3. Sky view factors calculated: (i) according to Johnson and Watson (1984), $\Psi_{equiangular}$, (ii) after correcting for lens-specific projection properties using (6), Ψ, and (iii) adjusting the latter for two different surface vapor pressure values for situations with strong inversion, Ψ_e, using (11). The factors were calculated retrieving the image in 2048 × 3072 pixels and dividing the image into 125 annuli.

Image	$\Psi_{Equiangular}$	Ψ	Ψ_5	Ψ_{20}
1	0.13	0.12	0.13	0.14
2	0.22	0.21	0.22	0.23
3	0.32	0.31	0.32	0.33
4	0.38	0.36	0.38	0.40
5	0.39	0.36	0.39	0.41
6	0.41	0.40	0.41	0.42
7	0.43	0.40	0.43	0.46
8	0.45	0.42	0.45	0.47
9	0.50	0.45	0.49	0.53
10	0.50	0.49	0.50	0.52
11	0.51	0.49	0.51	0.52
12	0.61	0.59	0.61	0.63
13	0.62	0.60	0.63	0.65
14	0.62	0.61	0.62	0.63
15	0.65	0.64	0.65	0.66
16	0.69	0.65	0.69	0.72
17	0.78	0.76	0.78	0.80
18	0.79	0.76	0.79	0.82
19	0.92	0.90	0.92	0.93
20	0.94	0.93	0.94	0.95

of the hemisphere near the horizon when used at an aperture setting of 5.6. This corresponds to a maximum sky view factor of less than 0.00003. For the environment where the photographs were taken, the sky close to the horizon was obscured, thus yielding a sky view factor of 0, which was used here for zenith angles between 89.7° and 90.0°.

5. Results

The sky view factor was calculated for 20 images: (i) according to Johnson and Watson (1984), $\Psi_{Equiangular}$, which for the number of annuli used here approximately equals the results from using the Steyn (1980) method, (ii) after correcting for lens specific projection properties using (6), Ψ, and (iii) adjusting the latter for two different surface vapor pressure values for situations with strong inversion using (11), Ψ_e (Table 3). The factors were calculated retrieving the image in the highest resolution (2048 × 3072 pixels) from the Kodak Photo CD and dividing the image into 125 annuli.

The sky view factor Ψ was calculated for various widths of annulus with the number of annuli n ranging from 1 to 1002 for an image retrieved in the highest resolution (Fig. 4). For three images retrieved in the five available resolutions, including the image used in Fig. 4, the sky view factor was calculated using the maximum number of annuli for each resolution (Table 4).

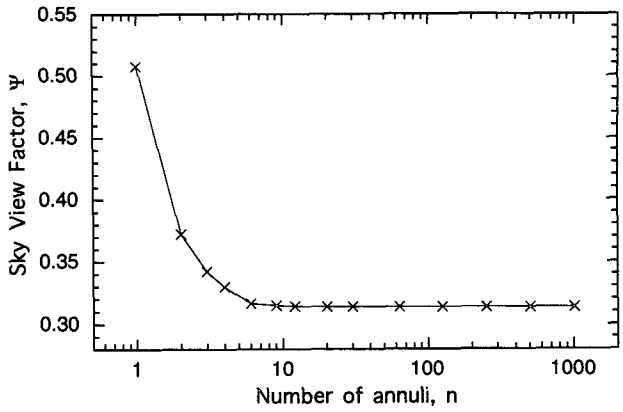

FIG. 4. The sky view factor Ψ calculated from the image reproduced in Fig. 3 retrieved within the highest resolution (array of 2048 × 3072 pixels) using various numbers of annuli for the calculation.

6. Discussion and conclusions

The method for analyzing photographic images that is presented here not only uses the more direct way of analyzing the image retrieved from the scanned negative, but also the Kodak Photo CD presents an easily accessible and compact way of storing large data quantities as produced by high-resolution scanning of negatives.

It is shown that deviations from perfectly equiangular projections and restrictions in field of view as produced by commercially available fish-eye lenses affect the results of view factor calculations. Simple methods to account for such deviations are presented. The Steyn (1980) and the Johnson and Watson (1984) methods overestimate the sky view factor when used on images produced with the Nikon 8-mm f/2.8 lens, which gives an approximate equiangular projection and only has a minor restriction in field of view (Table 3). Depending on the lens-specific angular calibration function, the bias is, however, likely to be even greater when using many other commercially available fish-eye lenses due to larger lens distortion (Herbert 1987). Also, the restriction in field of view for some commercially available fish-eye lenses is much larger than for the Nikon lens used in this study. Clark and Follin

TABLE 4. The sky view factor Ψ for three images, A–C, retrieved in five resolutions using the maximum number of annuli for each resolution, respectively. Image B corresponds to the image used in Figs. 3 and 4.

Pixel array	n	A	B	C
128 × 192	63	0.221	0.322	0.389
256 × 384	125	0.219	0.320	0.386
512 × 768	250	0.212	0.315	0.379
1024 × 1536	501	0.208	0.314	0.377
2048 × 3072	1002	0.205	0.313	0.377

(1988) report a field of view for the Sigma 8-mm, f/4 lens of only 160° although a 180° field of view is stated by the manufacturer. A reduced field of view not only produces images that are omitting parts of the hemisphere, but the diameter of the projected image on the negative corresponds to a solid angle of less than 180°, an angle that must be known when calculating the sky view factor.

Retrieving an image in high resolution makes the choice of threshold level less critical since aggregation of pixels to produce a smaller pixel array yields higher frequencies of "mixed pixels." This is especially important for calculating the sky view factor in complex environments such as beneath forest canopies. However, the number of annuli may be less than the maximum of 1002 at f/5.6 since the value for the sky view factor stabilizes when using more than about 20 annuli (Fig. 4). Using fewer annuli, each annulus spans a latitudinal angular width that is too wide to be represented by θ in (6). At 20 annuli, this gives a maximum error of less than 0.0008. A reasonable compromise between accuracy and time consumption for the calculation of sky view factors for complex environments would be to retrieve the image in 2048 × 3072 pixels and divide the image into about 20 annuli for the calculation. However, the results of the calculations are acceptable down to a resolution of 512 × 768 pixels, which also reduces the requirements on computer internal memory (Table 4).

The zenith angular variation of the atmospheric transmissivity to infrared radiation is shown to thoroughly affect the sky view factor. Hence, this variation should be considered when calculating the sky view factor for applications where the effective infrared radiation is of interest. In urban environments, special consideration may be needed for air pollutants that further reduce the transparency of the air to infrared radiation.

Acknowledgments. I would like to thank Professor Jan O. Mattsson, Department of Physical Geography, Lund University, Sweden, for valuable discussions; Dr. Kurth Perttu, Department of Ecology and Environmental Research, Swedish University of Agricultural Sciences, for lending the photographic equipment; Dr. P.-O. Zetterberg and his colleagues at the Department of Physics, Lund University, for valuable discussions and help with the laboratory setup for the tests with the Nikon lens; and Jonathan Seaquist for correcting the language. The work was supported by the Swedish Council for Planning and Coordination of Research, the Carl Trygger Foundation, the Royal Academy of Forestry and Agriculture, and the Swedish Society for Anthropology and Geography.

REFERENCES

Anderson, M. C., 1964: Studies of woodland light climate. I. The photographs of light conditions. *J. Ecol.*, **52,** 27–41.

Becker, P., D. W. Erhart, and A. P. Smith, 1989: Analysis of forest light environments. Part I. Computerized estimation of solar radiation from hemispherical canopy photographs. *Agric. For. Meteor.*, **44,** 217–232.

Blennow, K., 1994: Towards a general view factor and a view factor for effective infrared radiation applications. *Proc. IGU Conf. Contemporary Climatology,* Brno, Czech Republic., IGU, 61–66.

Bärring, L., J. O. Mattsson, and S. Lindqvist, 1985: Canyon geometry, street temperatures and urban heat island in Malmö, Sweden. *J. Climatol.*, **5,** 433–444.

Chan, S. S., R. W. McCreight, J. D. Walstad, and T. A. Spies, 1986: Evaluating forest vegetative cover with computerized analysis of fish-eye photographs. *For. Sci.*, **32,** 1085–1091.

Chen, J. M., T. A. Black, and R. S. Adams, 1991: Evaluation of hemispherical photography for determining plant area index and geometry of a forest stand. *Agric. For. Meteor.*, **56,** 129–143.

Clark, J. A., and G. M. Follin, 1988: A simple "equal area" calibration for fisheye photography. *Agric. For. Meteor.*, **44,** 19–25.

Eliasson, I., 1992: Infrared thermography and urban temperature patterns. *Int. J. Remote Sens.*, **13,** 869–879.

Evans, G. C., P. Freeman, and O. Rackham, 1975: Developments in hemispherical photography. *Light as an Ecological Factor: II,* C. G. Evans, R. Bainbridge, and O. Rackham, Eds., Blackwell, 549–556.

Herbert, T. J., 1986: Calibration of fisheye lenses by inversion of area projections. *Appl. Optics,* **25,** 1875–1876.

——, 1987: Area projections of fisheye photographic lenses. *Agric. For. Meteor.*, **39,** 215–233.

Johnson, G. T., 1990: Hemispherical density functions applied to video images. *Environ. Software,* **5,** 142–148.

——, and I. D. Watson, 1984: The determination of view-factors in urban canyons. *J. Climate Appl. Meteor.*, **23,** 329–335.

Monteith, J. L., 1961: An empirical method for estimating long-wave radiation exchanges in the British Isles. *Quart. J. Roy. Meteor. Soc.*, **87,** 171–179.

Nunez, M., and D. Sander, 1982: Protection from cold stress in a eucalyptus shelterwood. *J. Climatol.*, **2,** 141–146.

Oke, T. R., 1981: Canyon geometry and the nocturnal urban heat island: Comparison of scale model and field observations. *J. Climatol.*, **1,** 237–254.

Olsson, L., K. Carlsson, H. Grip, and K. Perttu, 1982: Evaluation of canopy photographs with diode-array scanner OSIRIS. *Can. J. For. Res.*, **12,** 822–828.

Reifsnyder, W. E., 1967: Radiation geometry in the measurement and interpretation of radiation balance. *Agric. For. Meteor.*, **4,** 255–265.

Steyn, D. G., 1980: The calculation of view factors from fish-eye lens photographs. *Atmos.–Ocean,* **18,** 254–258.

——, J. E. Hay, I. D. Watson, and G. T. Johnson, 1986: The determination of sky view factors in urban environments using video imagery. *J. Atmos. Oceanic Technol.*, **3,** 759–764.

Unsworth, M. H., and J. L. Monteith, 1975: Geometry of long-wave radiation at the ground. Part I: Angular distribution of incoming radiation at the ground. *Quart. J. Roy. Meteor. Soc.*, **101,** 13–24.